ARTICLE

Oxygen Reduction Reaction Activity of Fe-based Dual-Atom Catalysts with Different Local Configurations via Graph Neural Representation†

Xueqian Xia, Zengying Ma, Yucheng Huang*

College of Chemistry and Material Science, Key Laboratory of Functional Molecular Solids, Ministry of Education, Anhui Key Laboratory of Molecule-Based Materials, Anhui Carbon Neutrality Engineering Center, Anhui Normal University, Wuhu 241000, China

(Dated: Received on August 27, 2024; Accepted on September 13, 2024)

The performance of proton exchange membrane fuel cells depends heavily on the oxygen reduction reaction (ORR) at the cathode, for which platinum-based catalysts are currently the standard. The high cost and limited availability of platinum have driven the search for alternative catalysts. While FeN_4 single-atom catalysts have shown promising potential, their ORR activity needs to be further enhanced. In contrast, dual-atom catalysts (DACs) offer not only higher metal loading but also the ability to break the ORR scaling relations. However, the diverse local structures and tunable coordination environments of DACs create a vast chemical space, making large-scale computational screening challenging. In this study, we developed a graph neural network (GNN)-based framework to predict the ORR activity of Fe-based DACs, effectively addressing the challenges posed by variations in local catalyst structures. Our model, trained on a dataset of 180 catalysts, accurately predicted the Gibbs free energy of ORR intermediates and overpotentials, and identified 32 DACs with superior catalytic activity compared to FeN_4 SAC. This approach not only advances the design of high-performance DACs, but also offers a powerful computational tool that can significantly reduce the time and cost of catalyst development, thereby accelerating the commercialization of fuel cell technologies.

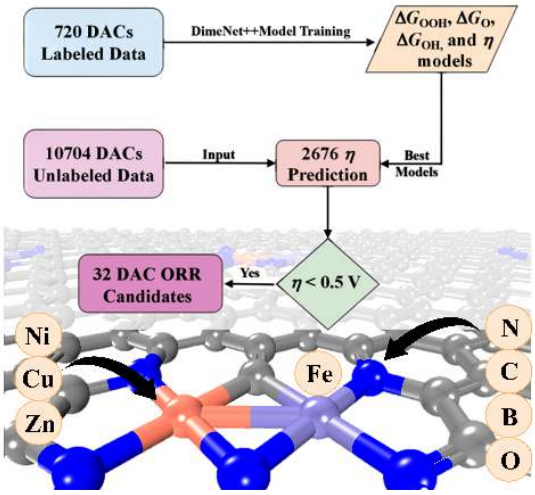

Key words: Oxygen reduction reaction, Dual-atom catalyst, Graph neural representation, Density functional theory, Artificial intelligence

I. INTRODUCTION

With the continuous growth of global energy demand, the development of clean and renewable energy technologies has become increasingly urgent [1–3]. Proton exchange membrane fuel cells (PEMFCs) have garnered significant attention as a promising energy conversion technology due to their high energy density, rapid refueling capability, and environmental friendliness [4, 5]. In the cathode of PEMFCs, the oxygen reduction reaction (ORR) is a pivotal electrochemical process, and its efficiency directly affects the overall performance of the cell [6, 7]. Although Pt-based catalysts are currently considered to be the most effective

† Part of Special Topic "Theoretical and Computational Catalysis".

* Author to whom correspondence should be addressed. E-mail: huangyc@mail.ahnu.edu.cn

ORR catalysts, their high cost and dependence on Pt resources limit their large-scale application [8, 9]. Consequently, the search for alternatives to Pt, particularly non-noble metal catalysts, has emerged as a research focal point. Single-atom catalysts (SACs), as a novel type of catalyst, have attracted widespread interest in reactions such as ORR due to their unique electronic and geometric structures, nearly 100% atomic utilization, high selectivity, and robust catalytic activity [10–14]. In particular, FeN_4 SACs are widely considered to be excellent ORR catalysts, but there is still room for further optimization of their activity [15, 16]. For instance, Li *et al.* [17] have successfully improved the ORR activity of FeN_4 by introducing Co single site into the second coordination shell.

Moreover, the quantity and activity of active sites are crucial in determining the catalytic performance [18, 19]. Dual-atom catalysts (DACs), which represent the ultimate limit of small-sized alloys due to their efficient utilization of metals, have attracted widespread attention [19–21]. Compared to SACs, DACs possess a greater number of metallic active sites, higher metal loading, and the ability to break the scaling relations of ORR and adjust the electronic structure of the catalyst. In recent years, the combination of density functional theory (DFT) calculations and machine learning (ML) methods has emerged as a powerful tool for screening and predicting high-performance bimetallic ORR catalysts. Zhao *et al.* [22] utilized a DFT-ML approach to evaluate the ORR and oxygen evolution reaction (OER) performance of 729 DACs containing 27 metal elements, identifying 30 DACs with ORR activity superior to Pt(111) and 10 DACs with OER activity better than RuO_2(110). The primary scientific challenge for bimetallic catalysts is the precise control of active site number and activity, alongside with the optimization of the electronic structure of the catalyst, to enhance catalytic performance. Traditional experimental methods have significant limitations in catalyst screening and optimization due to their high cost and time consumption. Although DFT calculations can provide atomic-level details, their substantial computational resource requirements preclude their use for large-scale catalyst screening. Therefore, the integration of DFT calculations and ML methods has become a powerful tool for addressing this critical scientific issue.

In this study, we introduce a graph neural network (GNN, DimeNet++ [23, 24])-based framework for predicting the ORR activity of Fe-based DACs. The innovation of this framework lies in its abilities to take the geometric structure of the catalyst as input and effectively handle DACs with varying configurations, which poses a challenge for traditional ML methods. In contrast to traditional feature-based algorithms, GNN has shown better performance and interpretability, due to the analogy between the constructed data structure and real geometric configurations and the introduction of message-passing processes [25]. As an advanced artificial intelligence technique, GNN possesses powerful spatial structure modeling capabilities and can learn the complex relationships between atoms, which is crucial for understanding catalyst activity. Utilizing the constructed GNN model, we can accurately predict the ORR activity of Fe-based DACs. The discovery of 32 DACs with overpotential lower than that of FeN_4 SAC highlights the potential for improved catalytic performance. Our research not only advances the development of clean energy technologies but also provides a novel and efficient computational tool for catalyst design, which is promising to significantly reduce the development cycle and cost of catalysts, ultimately promoting the commercialization process of fuel cell technology.

II. COMPUTATIONAL METHOD

All the spin-polarized calculations were carried out using the projector-augmented wave (PAW) [26] method as implemented in the Vienna Ab-initio Simulation Package [27]. We employed VASPKIT for the subsequent data processing [28]. The electron wave function was expanded with a plane-wave basis set with a cutoff energy of 400 eV. The generalized gradient approximation (GGA) [29] in the form of Perdew-Burke-Ernzerhof (PBE) [30] exchange-correlation functional was used. The Brillouin zone was sampled with a $3\times3\times1$ Γ-centered k-point grid following the scheme proposed by Monkhorst and Pack [31]. A vacuum space with thickness of 15 Å was applied along the c direction to avoid the interaction between two adjacent image layers. The DFT-D3 [32] method with the considering of van der Waals (vdW) corrections proposed by Grimme *et al.* was used. The conjugated gradient scheme was adopted for the geometric structure optimizations, and the convergence criterions for energy and force were set to be 10^{-5} eV and 10^{-2} eV/Å. All models were con-

DOI: 10.1063/1674-0068/cjcp2408114

structed based on a (3×6) graphene supercell with metal and nitrogen dopants. The Gibbs free energy change of chemical reaction is defined as follows:

$$\Delta G = \Delta E + \Delta \mathrm{ZPE} - T\Delta S$$

where ΔE is the reaction energy that can be obtained from DFT calculations, ΔZPE and ΔS represent the zero-point energy and the entropy change of each reaction step at temperature (T = 298.15 K), respectively.

III. RESULTS AND DISCUSSION

Although catalysts based on FeN_4 motifs have demonstrated excellent catalytic performance in ORR applications, their activity still falls short of the standards required for practical use [33, 34]. To further enhance the catalytic efficiency of the Fe sites, we considered the strategy of introducing diatomic sites, which not only maintains the stability of the Fe sites but also allows for fine-tuning of the ORR activity through the introduction of a second transition metal atom. In considerations of the economic viability and potential high-performance for practical applications, we selected three common transition metals: Ni, Cu, and Zn. Based on this strategy, we designed four representative diatomic FeM-NC configurations (DAC-A to DAC-D) as shown in FIG. 1. Among them, DAC-A, DAC-B, and DAC-C exhibit a FeM-N_6 coordination structure, while DAC-D presents a FeM-N_7 coordination environment. Previous studies have confirmed that the atoms in the first coordination sphere have a decisive influence on catalytic activity [35, 36]. Therefore, we precisely adjusted the metal coordination environment of the FeM-DAC by replacing the N atoms in the first coordination sphere with O/B/C atoms. This approach resulted in 2856 different configuration models, from which 180 catalyst structures were randomly selected for preliminary study and subjected to DFT calculations.

Building upon the established model, we further investigated the key determinant of catalyst reactivity: the adsorption energy of intermediates. In the ORR process, the OOH, O, and OH intermediates play crucial roles. Consequently, we conducted adsorption energy calculations for these critical intermediates on the 180 catalysts selected, amassing a dataset of 540 adsorption energy data points (FIG. 2). In FIG. 2(a), it can be observed that the values of ΔG_{OOH} are predominantly within the range of 2.5–4.0 eV. In FIG. 2(b),

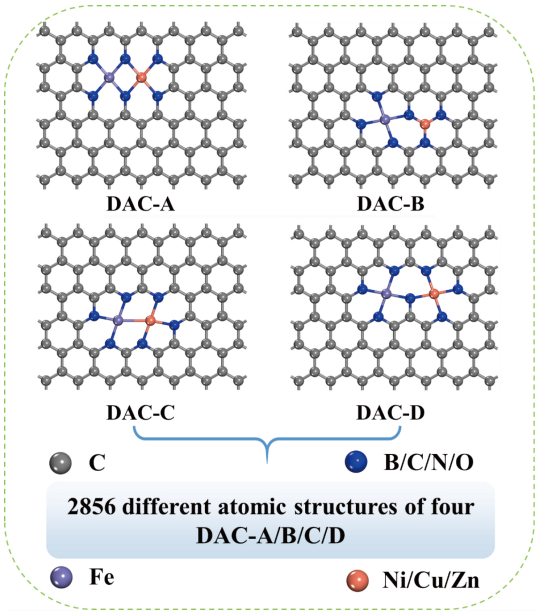

FIG. 1 Different structures of DACs.

ΔG_O values are mostly found between 0.5 and1.5 eV, while in FIG. 2(c), the majority of ΔG_{OH} values fall within 0–1 eV. The overpotential in ORR is of significant importance; therefore, we calculated the overpotential for the entire ORR hydrogenation reaction process. It was found that the overpotentials are largely within the range of 0.5–1 V, indicating that these catalysts exhibit poor ORR performance (FIG. 2(d)). Consequently, it is imperative to utilize machine learning methods to explore the entire chemical space in search of effective ORR catalysts.

Given the significant structural variations among the constructs, traditional descriptor methods and atom-based machine learning models were found to be inadequate in characterizing these structures. Therefore, we turned to the advanced technique of graph neural networks, which can convert atomic structures into graph representations, well-suited for handling the structural diversity present in our dataset. The basic principles and current application status of the GNN can be referred to a recent review article [37]. By applying DimeNet++ method, we were able to effectively capture and interpret the underlying chemical and catalytic features of these complex structures, providing profound insights and guidance for catalyst design and optimization. Moreover, the GNN model enables prediction of unknown catalyst structures, offering directions for experimental research and further advancing the development and application of ORR catalysts. FIG. 3 presents the training results for the adsorption free en-

DOI: 10.1063/1674-0068/cjcp2408114

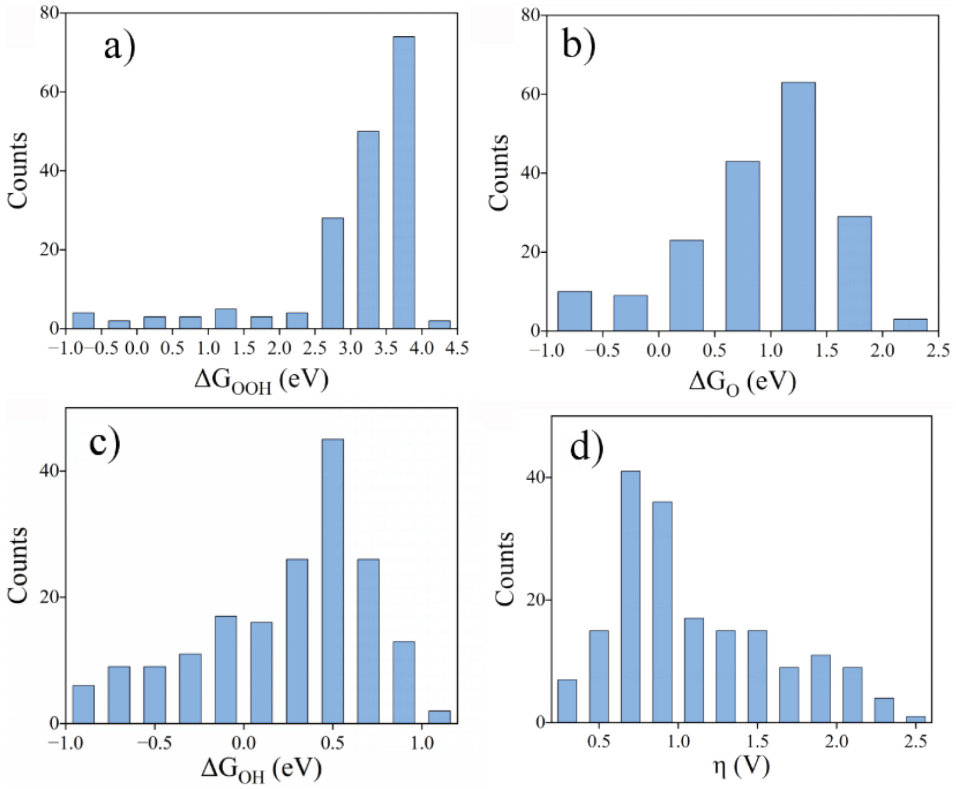

FIG. 2 The adsorption energy distributions of (a) ΔG_{OOH}, (b) ΔG_{O}, (c) ΔG_{OH}; and (d) overpotential η.

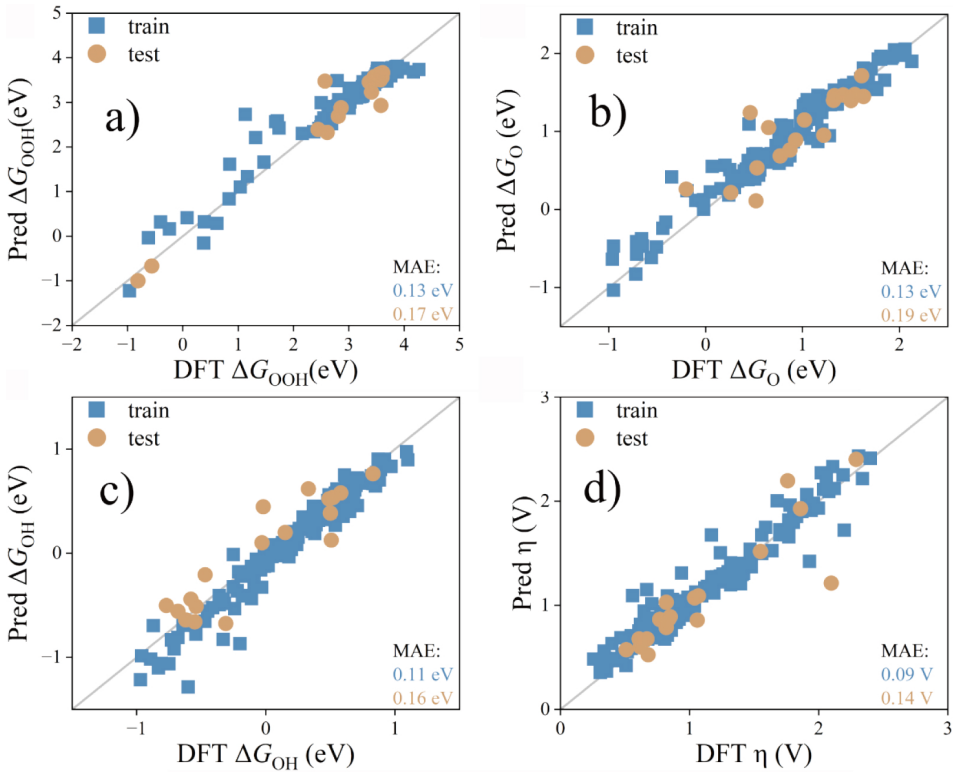

FIG. 3 The adsorption energy of (a) ΔG_{OOH}, (b) ΔG_{O}, (c) ΔG_{OH}, and (d) overpotential η with DFT and DimeNet++ prediction.

ergies of the OOH, O, and OH intermediates, as well as the overpotential, using the DimeNet++ model. We utilized unoptimized slab structures without intermediate adsorption as graph inputs, which significantly re-

DOI: 10.1063/1674-0068/cjcp2408114

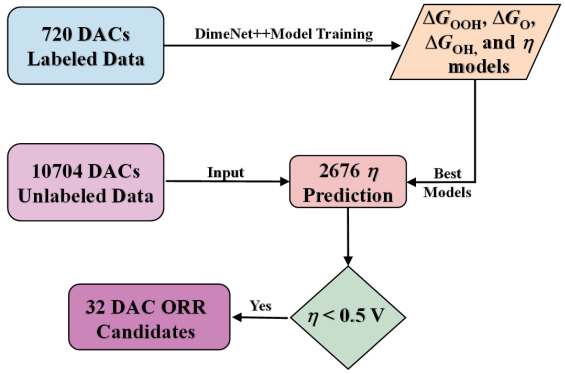

FIG. 4 The machine learning workflow screens for efficient Fe-based ORR DACs.

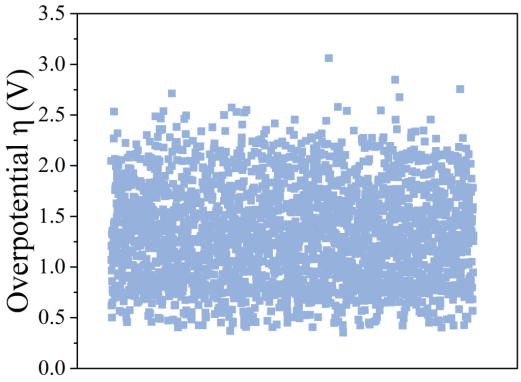

FIG. 5 Predicting the overpotential of catalysts across the entire search space.

duces computational effort compared to using optimized structures [38]. The adsorption energies and overpotential were targeted properties for dataset construction. Employing 10-fold cross-validation with the sklearn library [39], we achieved mean absolute errors (MAEs) of 0.13 eV for the training set and 0.17 eV for the test set on the OOH intermediate (FIG. 3(a)), indicating that the model is able to accurately predict ΔG_{OOH} on FeM DACs. FIG. 3 (b) and (c) show the Gibbs adsorption free energies for O and OH, with MAEs of 0.13 eV (0.19 eV) and 0.11 eV (0.16 eV) for the training (test) sets, respectively. Our machine learning outcomes suggest that the model effectively predicts the ORR reaction process on FeM DACs. Consequently, the overpotential, closely related to ORR activity, can also be predicted by our model. In FIG. 3(d), the MAEs for the overpotential on the training and test sets are 0.09 V and 0.14 V, respectively, demonstrating the capability of model in direct correlation with ORR performance.

The results show that our model can accurately predict the ORR activity of Fe-based DACs, facilitating the exploration of unlabeled chemical space. FIG. 4 outlines the machine learning workflow, starting with training the DimeNet++ model on 720 DFT data points to achieve high accuracy. This model was then used to predict the ORR intermediate Gibbs free energies of adsorption and overpotentials for the remaining 2676 structures.

The predictions for ΔG_{OOH}, ΔG_O, and ΔG_{OH} are shown in FIGs. S1–S3 (Supplementary materials, SM). FIG. 5 illustrates the predicted overpotentials for all unlabeled structures, where the majority of catalysts exhibit high values ranging from 1.0 V to 2.0 V. Notably, 32 FeN_4-based DACs demonstrate overpotential below the commonly reported theoretical ORR limit (0.5 V) of FeN_4 SAC [40, 41], indicating their potential for exceptional ORR activity. Generally, the C-, N-coordinated environment with the coordination number of 6 is more active. Among, the FeM-NC systems, especially their derived Janus structures, have been reported to behave excellent performance toward ORR recently [42].

IV. CONCLUSION

Utilizing the DimeNet++ approach with graph neural representations, we systematically investigated the ORR activities of 2856 Fe-based dual-atom catalysts with four distinct FeM-NX coordination environments. Employing a training set of 180 catalysts, totaling 540 adsorption energy data points and 180 overpotentials data points, we developed a robust machine learning model capable of accurately predicting Gibbs free energy data for ORR intermediates and overpotentials on FeM DACs. Our results indicate that 32 FeM DACs exhibit potential catalytic activity superior to FeN_4. Our findings provide support for the construction of machine learning models for DACs with various local structures and have identified a set of DACs with potential ORR activity, offering effective tools and methods for the advancement of DAC development.

Supplementary materials: The predicted ΔG_{OOH}, ΔG_O, ΔG_{OH} for 2676 FeM DACs are shown.

V. ACKNOWLEDGMENTS

This work was supported by the National Natural Science Foundation of China (No.22473001), the Natural Science Funds for Distinguished Young Scholar of Anhui Province (1908085J08), and the University An-

DOI: 10.1063/1674-0068/cjcp2408114

nual Scientific Research Plan of Anhui Province (2022AH010013).

[1] F. Liu and Z. X. Fan, Chem. Soc. Rev. **52**, 1723 (2023).
[2] Y. C. Wang, M. Zhang, Y. Y. Liu, Z. K. Zheng, B. Y. Liu, M. Chen, G. Q. Guan, and K. Yan, Adv. Sci. **10**, 2207519 (2023).
[3] P. P. Yang, X. Yang, W. Z. Liu, R. K. Guo, and Z. F. Yao, Green Energy Environ. **8**, 1265 (2023).
[4] E. L. Qu, X. F. Hao, M. Xiao, D. M. Han, S. Huang, Z. H. Huang, S. J. Wang, and Y. Z. Meng, J. Power Sources **533**, 231386 (2022).
[5] G. B. Zhang, Z. G. Qu, W. Q. Tao, X. L. Wang, L. Z. Wu, S. Y. Wu, X. Xie, C. Tongsh, W. M. Huo, Z. M. Bao, K. Jiao, and Y. Wang, Chem. Rev. **123**, 989 (2023).
[6] A. Dessalle, J. Quílez-Bermejo, V. Fierro, F. N. Xu, and A. Celzard, Carbon **203**, 237 (2023).
[7] P. B. Cui, L. J. Zhao, Y. D. Long, L. M. Dai, and C. G. Hu, Angew. Chem. Int. Ed. **62**, e202218269 (2023).
[8] X. R. Zhao and K. Sasaki, Acc. Chem. Res. **55**, 1226 (2022).
[9] Q. H. Shu, J. Zhang, B. Hu, X. Deng, J. L. Yuan, R. Ran, W. Zhou, and Z. P. Shao, Energy Fuels **36**, 1707 (2022).
[10] K. Liu, J. W. Fu, Y. Y. Lin, T. Luo, G. H. Ni, H. M. Li, Z. Lin, and M. Liu, Nat. Commun. **13**, 2075 (2022).
[11] Y. Q. Wang, J. Y. Hao, Y. Liu, M. Liu, K. Sheng, Y. Wang, J. Yang, J. Li, and W. Z. Li, J. Energy Chem. **76**, 601 (2023).
[12] B. Q. Ge, F. F. Wei, Q. Wan, H. W. Zhang, P. Yuan, and S. Lin, Precis. Chem. **1**, 429 (2023).
[13] K. X. Gu, H. Guo, and S. Lin, Angew. Chem. Int. Ed. **63**, e202405371 (2024).
[14] K. X. Gu and S. Lin, Angew. Chem. Int. Ed. **62**, e202312796 (2023).
[15] Y. Wang, Y. J. Tang, and K. Zhou, J. Am. Chem. Soc. **141**, 14115 (2019).
[16] Y. L. Han, Q. K. Li, K. Ye, Y. Luo, J. Jiang, and G. Z. Zhang, ACS Appl. Mater. Interfaces **12**, 15271 (2020).
[17] X. Y. Yi, H. J. Yang, X. X. Yang, X. K. Li, C. Yan, J. H. Zhang, L. N. Chen, J. J. Dong, J. Qin, G. N. Zhang, J. J. Wang, W. B. Li, Z. Y. Zhou, G. Wu, and X. F. Li, Adv. Func. Mater. **34**, 2309728 (2024).
[18] H. Chen, X. Liang, Y. P. Liu, X. Ai, T. Asefa, and X. X. Zou, Adv. Mater. **32**, 2002435 (2020).
[19] S. K. Singh, K. Takeyasu, and J. Nakamura, Adv. Mater. **31**, 1804297 (2019).
[20] J. Wang, C. X. Zhao, J. N. Liu, Y. W. Song, J. Q. Huang, and B. Q. Li, Nano Energy **104**, 107927 (2022).
[21] F. T. Wang, W. B. Xie, L. J. Yang, D. Q. Xie, and S. Lin, J. Catal. **396**, 215 (2021).
[22] Z. L. Fang, S. Y. Li, Y. J. Zhang, Y. X. Wang, K. Meng, C. Y. Huang, and S. R. Sun, J. Phys. Chem. Lett. **15**, 281 (2024).
[23] J. Klicpera, J. Groß, and S. Günnemann, *8th International Conference on Learning Representations*, Addis Ababa, (2020).
[24] J. Gasteiger, S. Giri, J. T. Margraf, and S. Günnemann, arXiv: 2011.14115 (2020).
[25] T. Xie and J. C. Grossman, Phys. Rev. Lett. **120**, 145301 (2018).
[26] P. E. Blöchl, Phys. Rev. B **50**, 17953 (1994).
[27] G. Kresse and J. Furthmüller, Phys. Rev. B **54**, 11169 (1996).
[28] V. Wang, N. Xu, J. C. Liu, G. Tang, and W. T. Geng, Comput. Phys. Commun. **267**, 108033 (2021).
[29] J. P. Perdew, K. Burke, and M. Ernzerhof, Phys. Rev. Lett. **77**, 3865 (1996).
[30] J. P. Perdew and Y. Wang, Phys. Rev. B **45**, 13244 (1992).
[31] H. J. Monkhorst and J. D. Pack, Phys. Rev. B **13**, 5188 (1976).
[32] S. Grimme, J. Antony, S. Ehrlich, and H. Krieg, J. Chem. Phys. **132**, 154104 (2010).
[33] J. C. Zhang, H. B. Yang, and B. Liu, Adv. Energy Mater. **11**, 2002473 (2021).
[34] Y. Yan, H. Y. Cheng, Z. H. Qu, R. Yu, F. Liu, Q. W. Ma, S. Zhao, H. Hu, Y. Cheng, C. Y. Yang, Z. F. Li, X. Wang, S. Y. Hao, Y. Y. Chen, and M. K. Liu, J. Mater. Chem. A **9**, 19489 (2021).
[35] L. B. Li, S. H. Huang, R. Cao, K. Yuan, C. B. Lu, B. Y. Huang, X. N. Tang, T. Hu, X. D. Zhuang, and Y. W. Chen, Small **18**, 2105387 (2022).
[36] Q. Z. An, S. W. Bo, J. J. Jiang, C. Gong, H. Su, W. R. Cheng, and Q. H. Liu, Adv. Sci. **10**, 2205031 (2023).
[37] P. Reiser, M. Neubert, A. Eberhard, L. Torresi, C. Zhou, C. Shao, H. Metni, C. van Hoesel, H. Schopmans, T. Sommer, and P. Friederich, Commun. Mater. **3**, 93 (2022).
[38] J. Gibson, A. Hire, and R. G. Hennig, npj Comput. Mater. **8**, 211 (2022).
[39] L. Buitinck, G. Louppe, M. Blondel, F. Pedregosa, A. Mueller, O. Grisel, V. Niculae, P. Prettenhofer, A. Gramfort, J. Grobler, R. Layton, J. Vanderplas, A. Joly, B. Holt, and G. Varoquaux, arXiv: 1309.0238 (2013).
[40] H. Xu, L. H. Xiao, P. X. Yang, X. Y. Lu, L. L. Liu, D. Wang, J. Q. Zhang, and M. Z. An, J. Colloid Interface Sci. **638**, 242 (2023).
[41] Z. P. Miao, X. M. Wang, M. C. Tsai, Q. Q. Jin, J. S. Liang, F. Ma, T. Y. Wang, S. J. Zheng, B. J. Hwang, Y. H. Huang, S. J. Guo, and Q. Li, Adv. Energy Mater. **8**, 1801226 (2018).
[42] C. Brea and G. X. Hu, ACS Catal. **13**, 4992 (2023).

DOI: 10.1063/1674-0068/cjcp2408114